Cell Stress and Chaperones (2016) 21:313–326
DOI 10.1007/s12192-015-0661-5

ORIGINAL PAPER

Structural studies of UBXN2A and mortalin interaction and the putative role of silenced UBXN2A in preventing response to chemotherapy

Sanam Sane[1] · Ammara Abdullah[1] · Morgan E. Nelson[1] · Hongmin Wang[1] · Subhash C. Chauhan[2] · Samuel S. Newton[1] · Khosrow Rezvani[1]

Received: 4 August 2015 / Revised: 16 November 2015 / Accepted: 18 November 2015 / Published online: 4 December 2015

Abstract Overexpression of the oncoprotein mortalin in cancer cells and its protein partners enables mortalin to promote multiple oncogenic signaling pathways and effectively antagonize chemotherapy-induced cell death. A UBX-domain-containing protein, UBXN2A, acts as a potential mortalin inhibitor. This current study determines whether UBXN2A effectively binds to and occupies mortalin's binding pocket, resulting in a direct improvement in the tumor's sensitivity to chemotherapy. Molecular modeling of human mortalin's binding pocket and its binding to the SEP domain of UBXN2A followed by yeast two-hybrid and His-tag pull-down assays revealed that three amino acids (PRO442, ILE558, and LYS555) within the substrate-binding domain of mortalin are crucial for UBXN2A binding to mortalin. As revealed by chase experiments in the presence of cycloheximide, overexpression of UBXN2A seems to interfere with the mortalin-CHIP E3 ubiquitin ligase and consequently suppresses the C-terminus of the HSC70-interacting protein (CHIP)-mediated destabilization of p53, resulting in its stabilization in the cytoplasm and upregulation in the nucleus. Overexpression of UBXN2A causes a significant inhibition of cell proliferation and the migration of colon cancer cells. We silenced UBXN2A in the human osteosarcoma U2OS cell line, an enriched mortalin cancer cell, followed by a clinical dosage of the chemotherapeutic agent 5-fluorouracil (5-FU). The UBXN2A knockout U2OS cells revealed that UBXNA is essential for the cytotoxic effect achieved by 5-FU. UBXN2A overexpression markedly increased the apoptotic response of U2OS cells to the 5-FU. In addition, silencing of UBXN2A protein suppresses apoptosis enhanced by UBXN2A overexpression in U2OS. The knowledge gained from this study provides insights into the mechanistic role of UBXN2A as a potent mortalin inhibitor and as a potential chemotherapy sensitizer for clinical application.

Keywords Mortalin · UBXN2A · p53 · Chemotherapy · Osteosarcoma · Colon cancer

Introduction

Mortalin-2/Grp75/HSPA9B/mot-2 (mortalin) is a member of the heat shock protein 70 (HSP70) family (Wadhwa et al. 1993b). Mortalin does not quite fit with other members of the HSP70 family due to its non-inducibility to heat shocks (Kaul et al. 2007). Besides inactivation of p53 during the progression of cancer (Lu et al. 2011; Sane et al. 2014). mortalin enhances cancer proliferation and metastasis through other pathways as follows: (i) Mortalin negatively regulates the Raf/MEK/ERK pathway, which triggers innate tumor-suppressive mechanisms. In fact, inhibition of mortalin increases $p21^{CIP1}$ transcription and MEK/ERK activity, which

Electronic supplementary material The online version of this article (doi:10.1007/s12192-015-0661-5) contains supplementary material, which is available to authorized users.

✉ Khosrow Rezvani
khosrow.rezvani@usd.edu

[1] Division of Basic Biomedical Sciences, Sanford School of Medicine, The University of South Dakota, 414 E. Clark Street, Lee Medical Building, Vermillion, SD 57069, USA

[2] Department of Pharmaceutical Sciences and Center for Cancer Research, University of Tennessee Health Science Center, Memphis, TN, USA

leads to cell death and growth arrest in MEK/ERK-activated cancer cell lines (Wu et al. 2013). (ii) Mortalin inhibits the pro-apoptotic Bax protein in both p53-dependent and p53-independent manners (Lu et al. 2011; Yang et al. 2011). (iii) In addition to its cytoplasmic sequestration and inactivation of p53, a recent report indicated that in cancer cells mortalin localizes in the nucleus and inactivates p53-mediated control of centrosome duplication, causing genomic instability. In addition, mortalin nuclear localization leads to the activation of hTERT (a telomere-maintaining enzyme) and hnRNP-K (a multifunctional chromatin-remodeling protein). The hTERT and hnRNP-K promote carcinogenesis (Ryu et al. 2014). (iv) Current evidence indicates mortalin contributes to the epithelial-to-mesenchymal transition, a crucial step in tumor invasion and metastasis (Chen et al. 2014). as well as angiogenesis (Yoo et al. 2010) during the progression of a tumor. (v) Finally, there is evidence that mortalin associates with DJ-1 protein and they coordinately maintain cancer stem cells through the control of oxidative stress (Conte et al. 2009; Tai-Nagara et al. 2014). Taken together, the above evidence illustrates that mortalin plays an important and distinct role in tumorigenesis and metastasis in several cancers, including colon, brain, and osteosarcoma cancers (Kaul et al. 2007; Wadhwa et al. 2006). Therefore, mortalin is a potential therapeutic target for a subset of cancers possessing upregulated mortalin.

We discovered UBXN2A binds to and inactivates mortalin. By binding to mortalin, UBXN2A reactivates wild-type (WT)-p53 tumor suppressor protein (Sane et al. 2014) and induces apoptosis at the cellular level and in tumor xenografts (Abdullah et al. 2015b). In addition, we discovered that induction of UBXN2A by its enhancer (Abdullah et al. 2015a). Veratridine, can synergistically enhance the effectiveness of the chemotherapeutic agents etoposide and 5-fluorouracil (5-FU), particularly in well-differentiated colon cancer cells.

In this current study, we first employed a combination of computational structural approaches and protein-protein docking studies followed by genetic and biochemical approaches to further determine the molecular mechanism of UBXN2A-mortalin interaction. These experiments revealed that the SEP (*Saccharomyces cerevisiae*, *Drosophila melanogaster eyes* closed gene, and vertebrate 47) domain (Soukenik et al. 2004) of UBXN2A binds partially to mortalin's binding pocket located within the SBD (substrate-binding domain), and three amino acids (PRO442, ILE558, and LYS555) could be essential for this interaction. A series of cell-based assays verified UBXN2A expression, and its consequent binding to mortalin can reverse cell proliferation, anti-apoptosis, and migration promoted by the cytoplasmic mortalin in the colon and U2OS cancer cell lines. Gain- and loss-of-UBXN2A experiments showed UBXN2A positively mediates apoptosis events in cancer cells, and its presence is essential for the induced cytotoxic effect of 5-FU.

Material and methods

Molecular modeling The amino acid sequence of mortalin (AAH24034.1) containing 679 residues was used to obtain homologous templates in the SWISS-MODEL homology-modeling server (Arnold et al. 2006; Biasini et al. 2014). Templates were chosen based on high homology (62 % amino acid sequence identity) and available high-resolution X-ray crystal structure (Fig. 1 supplementary). Automated model building was performed by the SWISS-MODEL server. Models were examined for accuracy by comparison with the 2.8-Å crystal structure of the nucleotide-binding domain of mortalin (PDB entry 4KBO). Hydrogens were added and side chains were optimized using a rotamer library (SCWRL), steepest descent, and semi-empirical quantum mechanics (MOPAC) in YASARA Structure (Krieger et al. 2012; Krieger and Vriend 2015). The homology model was inspected and validated using the protein structure validation suite (Bhattacharya et al. 2007). The entire structure was subjected to molecular dynamics simulation in YASARA. The simulation cell was filled with water and run at 298 K using the AMBER force field. A similar approach was used to generate the homology model of the SEP domain of UBXN2A. The solution structure of human p47 (PDB entry 1SS6) was used as the template. Docking of mortalin and the UBXN2A SEP domain was performed using the ClusPro 2 server (Boston University) (Comeau et al. 2004; Kozakov et al. 2013). Only structures that scored in the top 2 were considered. Figures were prepared using PyMol.

Antibodies Table 1 in Supplemental Material (online resources) lists primary antibodies and the titers used for western blotting (WB). The sequences of primers used will be provided upon request.

Cell culture, generation of cell lines, chemicals, and drug treatments Human HEK-293T cells, human HCT-116 and LoVo colon cancer cells, and human U2OS osteosarcoma cells were obtained from the ATCC (American Type Culture Collection). All cells were grown in their appropriate mediums supplemented with 10 % fetal bovine serum (Life Technologies, Grand Island, NY) at 37 °C in the presence of 5 % CO2. The $(His)_6$-TYG-tagged human UBXN2A in pcDNA3.1Z+ expression vector and a negative expression control vector (pcDNA3.1/Zeo) were transiently co-transfected with pCMV-HA-N (Clontech, Mountain View, CA) empty vector or pCMV-HA-N containing SBD or a mutant form of SBD (Fig. 3) using Lipofectamine 2000 (Life Technologies). In a set of experiments, $(His)_6$-TYG-tagged UBXN2A or GFP-UBXN2A cloned in pAcGFP1-C1 (Clontech, Mountain View, CA) (Sane et al. 2014) were co-transfected with $(His)_6$-CHIP E3 ubiquitin ligase followed by

WB analysis or immunocytochemical (Sane et al. 2014) detection of p53.

Cell proliferation assay Transiently transfected HCT-116 colon cancer cells with $(His)_6$-TYG-empty or $(His)_6$-TYG-UBXN2A vectors were seeded (1000 cells per well) in 96-well plates for 24-, 48-, 72-, and 96-h time points. MTT (3-[4, 5-dimethylthiazolyl-2]-2, 5-diphenyltetrazolium bromide) (CellTiter 96 AQeous One Solution Cell Proliferation Assay, Promega, Madison, WI) reagent was added to each well of the plates 2 h before the end of each time point and incubated at 37 °C. The color intensity (absorbance) was measured at 490 nm using a microplate reader (BioMate 3 UV-Vis spectrophotometer, Thermo Electron Corporation, Waltham, MA). The absorbance values obtained were plotted against each time point.

Colony formation assay Transfected HCT-116 cells expressing $(His)_6$-TYG-tagged UBXN2A or $(His)_6$-TYG-tagged empty vector were selected with Zeocin (100 μg/ml) for 2 days as described previously (Sane et al. 2014). Transfected cells were seeded (1000 cells per disc) in a 100-mm culture disc for 9 days for cells to form colonies. At the 5th day, media was replaced with fresh media. After 9 days, the cells were washed twice with PBS, fixed with 70 % ethanol, stained with hematoxylin (Fisher Scientific, Pittsburgh, PA), and further washed with water and air-dried. Colonies containing more than 50 cells were considered well-formed colonies. The colonies were imaged and counted with a Multimage™ Cabinet (Alpha Innotech Corporation, San Leandro, CA) using AlphaEaseFC software. The average number of colonies was plotted for HCT-116 vector and HCT-116 UBXN2A-expressing cells.

Migration assay For the migration assay, 1000 cells were seeded into an ibidi plate with two chambers (single culture-insert in a 35-mm μ-dish, ibidi USA, Inc.). After 24 h, LoVo and HCT-116 colon cancer cells were transfected with GFP-empty or GFP-UBXN2A vector (Sane et al. 2014). After another 24 h, inserts were removed, creating a gap of ~500 μm. The well was filled with proper medium and cells were allowed to grow for another 24 h. The number of migrated cells within the gap was counted in 11 random areas by live cell imaging at ×10 magnification with bright-field and GFP acquisitions using a Zeiss motorized inverted microscope and measuring the number of migrated cells using AxioVision software. Migrated cells were analyzed using GraphPad Prism 6.

Yeast two-hybrid, flow cytometry (Annexin V, Caspase-3 and cleaved PARP), immunocytochemistry, and His-tag pull-down assays These four assays were conducted as previously described (Abdullah et al. 2015a; Rezvani et al. 2009, 2012; Sane et al. 2014).

Statistical analysis of data Unless otherwise indicated, at least three biological repeats were performed for all the cell culture experiments. Statistical values were analyzed with either Student's *t* test or by one-way ANOVA and Tukey multiple comparison post hoc tests, using GraphPad Prism 6 when appropriate. The means were compared considering a p value of ≤ 0.05 as a significant difference (mean±SEM).

Results

Molecular modeling of mortalin

The homology model of mortalin shows the nucleotide-binding domain and the substrate-binding domain linked by a bridge and producing a cleft (Fig. 1a, b). The last three amino acids (PRO442, LYS555, and ILE558) used by p53 (Iosefson and Azem 2010; Utomo et al. 2012) can be seen adjacent to this cleft. This model enabled us to further examine the structural relationship between mortalin and UBXN2A by protein-protein docking. Docking analysis showed the SEP domain engaging this pocket in a region close to the above three residues (Fig. 1c, d).

UBXN2A binds to mortalin's binding pocket within the substrate-binding domain of mortalin

Our previously published results showed the SEP domain of UBXN2A is sufficient to interact with WT-mortalin. The truncated mortalin proteins confirmed a partial section of the mortalin binding pocket on the SBD domain of mortalin (aa 438–506) is sufficient for binding to WT-UBXN2A (Sane et al. 2014). Interestingly, the p53 binding site of mortalin is also located within the substrate-binding domain (SBD domain) in the range of 423 to 450 residues, while 7 amino acids (THR433, VAL435, LEU436, LEU437, PRO442, ILE558, and LYS555) mediate p53 and mortalin interaction (Iosefson and Azem 2010; Utomo et al. 2012). Based on the above information, we initially concluded that the first four residues (THR433, VAL435, LEU436, and LEU437) within the mortalin pocket are not essential for UBXN2A interaction. Because UBXN2A can displace p53 from mortalin (Sane et al. 2014). we hypothesized that a part of the mortalin binding pocket and the last three amino acids used by p53 (PRO442, ILE558, and LYS555) can be important for SEP domain binding.

To confirm whether the three amino acids PRO(P)442, ILE(I)558, and LYS(K)555 can in fact play a role for UBXN2A-mortalin interaction similar to p53-mortalin interaction, we employed a yeast two hybrid (Y2H) technique (Rezvani et al. 2009; Sane et al. 2014). cDNAs of human UBXN2A and wild-type (WT)-mortalin or the SBD domain of mortalin were cloned into the pGBKT7 DNA-binding

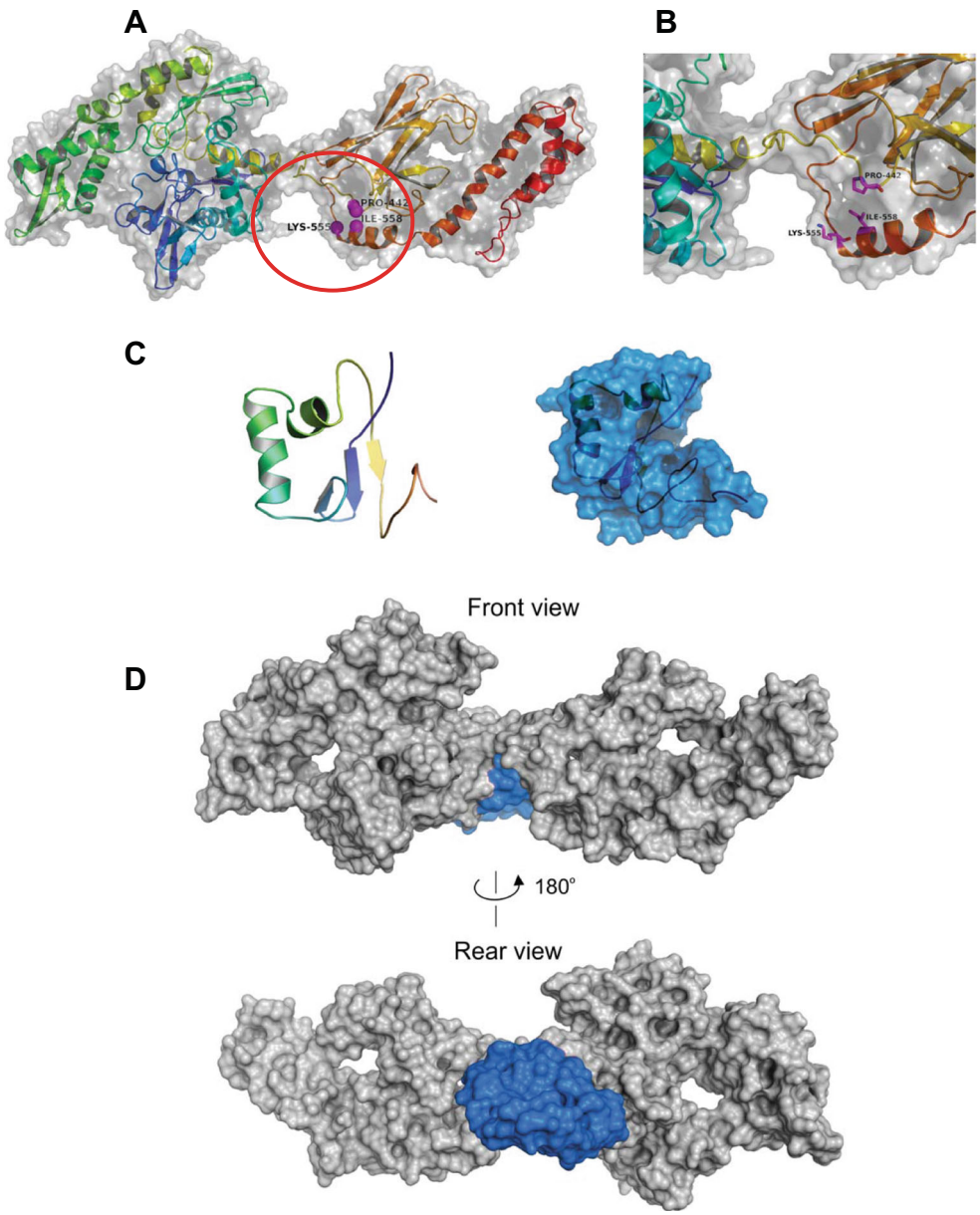

Fig. 1 Structure of mortalin and the underlying topology of the UBXN2A-mortalin complex. **a** Homology model of mortalin showing ATPase (*left*) and substrate-binding (*right*) domains. Molecular surface is shown in *transparent gray*. The locations of critical amino acid residues involved in UBXN2A binding are indicated by *purple spheres*. **b** The region connecting both domains is shown in close-up view. Side chains of P442, K555, and I558 are in a cleft of the substrate-binding domain. **c** Homology model of the SEP (after shp1, eyc, and p47) domain of UBXN2A is shown in *ribbon conformation* and a *blue transparent molecular surface*. **d** Docking of mortalin (*gray molecular surface*) and SEP domain of UBXN2A (*blue molecular surface*). The same view as in **a** is shown in the *top panel* of **d**. The structure is rotated 180° in the lower panel to show the rear view and the location of SEP domain binding. This computational study explains the topological properties of mortalin which allow UBXN2A-mortalin interaction

domain (bait plasmid, Clontech) and pGAD10 DNA activation domain (prey plasmid, Clontech) vectors, respectively (Fig. 2a, b). The QuikChange Site-Directed Mutagenesis Kit (Agilent Technologies, Santa Clara, CA) allowed us to introduce four different point mutations within the SBD domain of mortalin as follows: T441A, P442A, K555A, and I558A. The proline (P), lysine (K), and isoleucine (I) amino acids mutated to alanine are those potential residues characterized by computational studies. In addition, we mutated T441 (threonine) amino acid to alanine to be used as a control mutant (Fig. 2b). Yeast AH109 containing wild-type (WT) UBXN2A and its mating partner, pGAD10, containing mortalin, SBD, or point-mutated SBD constructs were mated together, and the resulting diploid yeasts were selected based on nutritional selections (Ade, His, Leu, and Trp). The positive protein-protein interactions were further examined on plates containing X-α-Gal for the colorimetric detection of the MEL1 reporter gene product α-galactosidase. This triple selection (Ade, His, MEL1) method showed WT-UBXN2A binds to both mortalin and the SBD domain. However, mutation of P442, K555, or I558 to alanine disrupted UBXN2A-SBD interaction (Fig. 2c). Mutation of T441 (control mutant) to alanine did not interfere with UBXN2A-SBD interaction (Fig. 2c). Taken together, these results indicate that UBXN2A binds to and occupies the mortalin binding pocket and UBXN2A partially shares the amino acid binding site with p53 protein. In addition, these genetic approaches further confirmed the protein-protein docking model described in Fig. 1.

In the second set of experiments, we transformed SBD domain and point-mutated SBD constructs from the yeast

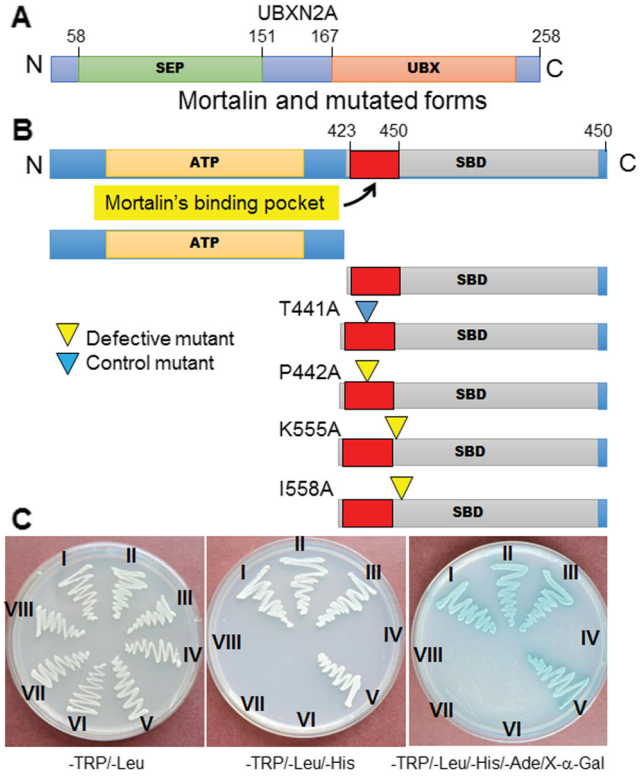

Fig. 2 UBXN2A binds to mortalin's binding pocket within the substrate-binding domain of mortalin. **a** This schematic diagram shows the SEP (Shp, eyes closed, p47 in bold) domain, located in the N-terminus of UBXN2A, and the UBX (ubiquitin-regulatory X in bold) domain, located in the C-terminus of UBXN2A protein. **b** Structure of mortalin's functional domains, including an ATPase domain at the N-terminus of mortalin protein and a substrate-binding domain (SBD) located in the C-terminus of mortalin protein. Wild-type, truncated ATP, and SBD domains as well as SBD mutant (T441A, P442A, K555A, and I558A) forms of mortalin were cloned into the yeast pGAD10 DNA activation vector. The cDNA of wild-type UBXN2A was cloned into the yeast pGBKT7 DNA-binding domain vector. The SBD mutant forms of mortalin were generated according to the molecular docking results. **c** We conducted a set of Y2H assays using WT-mortalin and UBXN2A as well as truncated and point-mutated forms of mortalin protein. Our results confirmed that the mutation of three specific amino acids (PRO442, LYS555 and ILE558) predicted by the structural studies can block UBXN2A from binding to the SBD domain of mortalin based on nutritional selection and α-galactosidase assays. *I*, p53-SV40 (positive control); *II*, WT-UBXN2A-WT-mortalin; *III*, WT-UBXN2A-SBD domain; *IV*, WT-UBXN2A-ATP domain; *V*, WT-UBXN2A-SBD (T441A); *VI*, WT-UBXN2A-SBD (P442A); *VII*, WT-UBXN2A-SBD (K555A); *VIII*, WT-UBXN2A-SBD (I558A)

pGAD10 vector to its compatible mammalian vector pCMV-HA-N. HEK-293T cells were co-transfected with $(His)_6$-TYG-UBXN2A (Sane et al. 2014) and pCMV-HA-N containing SBD domain or point-mutated SBD constructs (Fig. 3a). Twenty-four hours after transient transfection, total cell lysates were subjected to magnetic His-tag beads (Sane et al. 2014) to isolate the UBXN2A protein and its partners. Similar to the Y2H results, WB analysis showed UBXN2A was able to successfully pull down the un-mutated SBD domain (Fig. 3b). However, UBXN2A failed completely (P442A and I558A) or partially (K555A) to pull down the point-mutated form of SBD domain (Fig. 3b). Combining the computational study with the Y2H and His-tag pull-down assays indicates that UBXN2A binds to and occupies the mortalin binding pocket within the SBD domain. As previously described (Wadhwa et al. 2015). there are individual amino acids within mortalin whose mutations can dramatically change mortalin functions, including alteration in mortalin binding partners. The above experiments suggest that the presence of PRO442, LYS555, and ILE558 amino acids are necessary when UBXN2A binds to the SBD domain of mortalin.

UBXN2A increases stability of p53 protein targeted by the mortalin-CHIP E3 ubiquitin ligase

During cell stress, the C-terminus of the HSC70-interacting protein (CHIP) E3 ubiquitin ligase preferentially targets and ubiquitinates chaperone-bound substrates attached to heat shock protein 70 (HSP70) for proteasomal degradation (Qian et al. 2006). One example is p53, which is targeted by the HSP70-CHIP complex for ubiquitination and proteasomal degradation (Lee and Gu 2010) in normal cells under post-stress conditions. As a subgroup of the HSP70 family, mortalin also binds to CHIP protein in the cytoplasm (Kaul et al. 2007). In addition, we have previously shown UBXN2A binds and negatively regulates CHIP at the endoplasmic reticulum (ER) level as part of ER-associated degradation (ERAD) pathway (Teng et al. 2015). Additional experiments are ongoing in our group to determine whether mortalin-CHIP interaction is direct or indirect. It has been suggested that CHIP binds to mortalin and mediates proteasomal degradation of selective substrates such as p53 (Kaul et al. 2007). In fact, overexpression of mortalin decreases the protein level of p53 in U2OS cells (Wadhwa et al. 2015). To test whether UBXN2A can inhibit mortalin/CHIP-dependent degradation of p53 in the cytoplasm, we transiently transfected HEK293T cells with $(His)_6$-CHIP E3 ubiquitin ligase±GFP-empty or GFP-UBXN2A (see "Material and methods" section). Twenty-four hours after transfection, cells were treated with cycloheximide (CHX, 0.1 mg/ml) for 2 h (Yuan et al. 2010). Total cell lysates were prepared, followed by WB analysis. As previously described (Esser et al. 2005). overexpression of CHIP decreases p53 levels (Fig. 3c, lane 2 versus 1). Interestingly, expression of exogenous UBXN2A reverses CHIP-dependent degradation of p53 (Fig. 3c, lane 3 versus 2). As previously shown (Sane et al. 2014). overexpression of UBXN2A alone led to a mild elevation of p53 in the cytoplasm (Fig. 3c, lane 4 versus 1). Quantitation of the p53 signals of three independent WB experiments (Fig. 3c) indicated that UBXN2A overexpression can disrupt recruitment and degradation of p53 by the CHIP protein, allowing p53 stabilization.

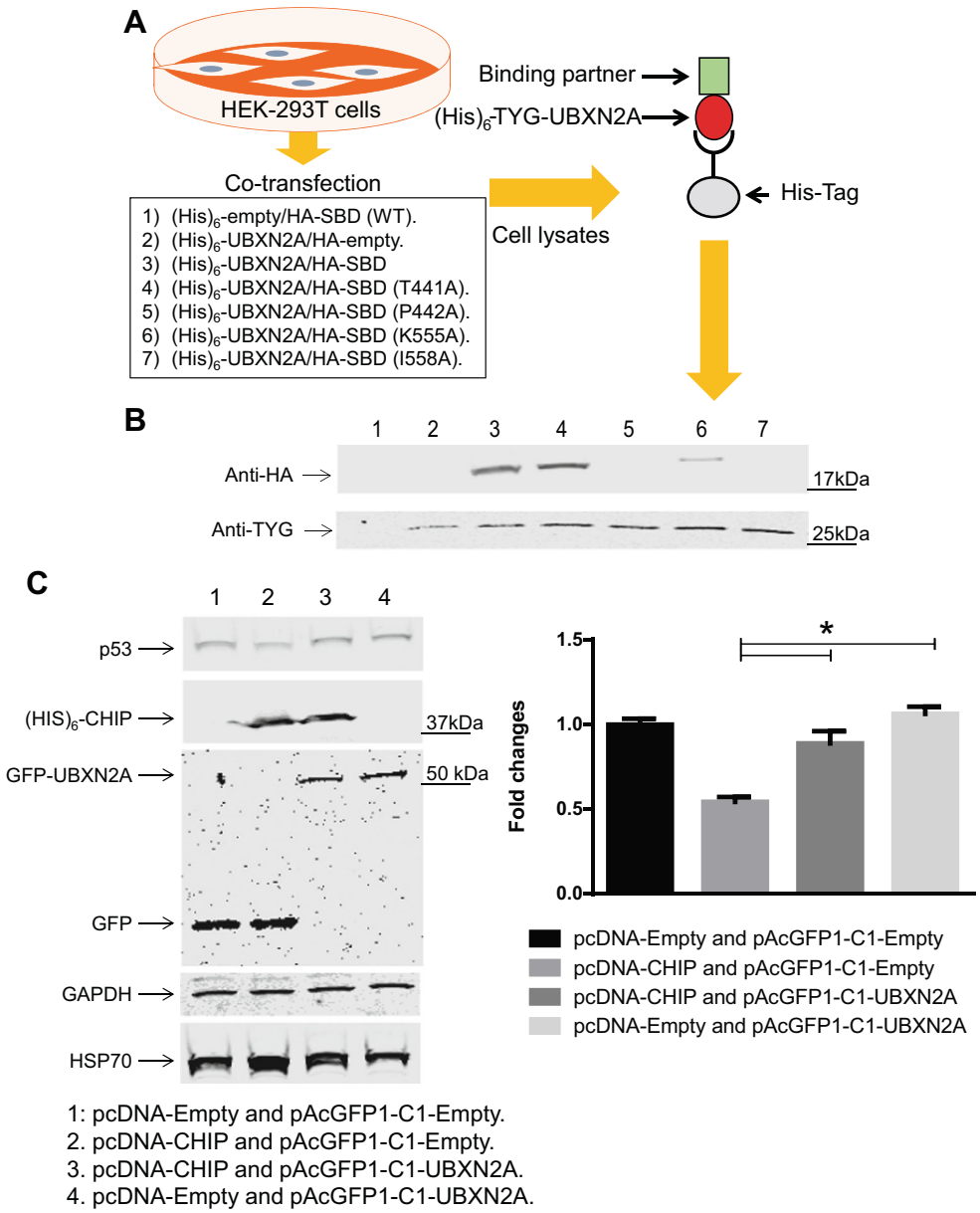

Fig. 3 Analysis of UBXN2A-SEP interactions in HEK-293T cells. **a** HEK-293T cells were co-transfected with the indicated expression vectors. Twenty-four hours after transfection, cell lysates were prepared. **b** We used the Dynabeads® magnetic His-Tag bead-based technology to pull down $(His)_6$-UBXN2A and its binding partners followed by WB analysis using anti-HA and anti-TYG antibodies. Anti-HA antibody detected SBD and SBD mutants (upper panel) and anti-TYG antibody detected $(His)_6$-UBXN2A protein. Both WT-HA-SBD and HA-SBD (T441A) were pulled down by $(His)_6$-UBXN2A. However, mutation of three amino acids (P-442, K-555, and I-558) located in the SBD domain eliminated completely (P and I amino acids) or partially (L amino acid) UBXN2A binding to the binding site pocket of SBD. These His-tag pull-down experiments verified the Y2H results provided in Fig. 2 and indicate a direct physical binding between UBXN2A and the SBD domain. **c** Another set of experiments was designed to examine whether UBXN2A can functionally disrupt degradation of p53 mediated through the cytoplasmic mortalin-CHIP complex. HEK293T cells were co-transfected with $(His)_6$-CHIP and GFP-empty or GFP-UBXN2A. Twenty-four hours after transfection, cells were treated with CHX for 2 h and total cell lysates were prepared for WB analysis. Results showed overexpression of CHIP decreased p53 levels in the cytoplasm. In contrast, overexpression of UBXN2A neutralized CHIP-dependent destabilization of p53. UBXN2A overexpression alone had no dramatic effect on total p53 levels, as previously observed in the HCT-116 colon cancer cell line (Sane et al. 2014). The *bar graph* shows a quantitation of p53 signals pooled from three independent experiments. By binding to mortalin, UBXN2A may antagonize CHIP-dependent destabilization of p53, suggesting a novel regulatory mechanism for CHIP-E3 ubiquitin ligase activity

It has been previously illustrated that inhibition of mortalin leads to activation and relocation of p53 to the nucleus (Kaul et al. 2005; Lu et al. 2011). To examine whether the UBXN2A-dependent inhibition of CHIP and stabilization of p53 in the cytoplasm observed in Fig. 3c can lead to p53 nuclear localization, we transiently transfected HEK293T cells with $(His)_6$-

empty or $(His)_6$-TYG-UBXN2A vector±$(His)_6$-CHIP. Twenty-four hours after transfection, cytoplasmic and nuclear cell lysates (Abdullah et al. 2015a) were prepared, followed by WB analysis. Overexpression of CHIP decreases p53 levels in both the cytoplasm and nucleus (Fig. 2a supplementary, lane 2 versus 1) while expression of exogenous UBXN2A reverses CHIP-dependent degradation of p53, particularly in the nucleus (Fig. 2a supplementary, lane 3 versus 2). Overexpression of UBXN2A alone led to a moderate elevation of p53 in both cytoplasmic and nuclear fractions (Fig. 2a supplementary, lane 4 versus 1). This set of experiments indicates that, by binding to mortalin, UBXN2A overexpression may disrupt recruitment and degradation of p53 by the mortalin-CHIP complex, allowing p53 stabilization and nuclear localization. A set of immunocytochemistry experiments using LoVo colon cancer cells transiently transfected with GFP-UBXN2A confirmed nuclear localization of p53 in the presence of UBXN2A in the cytoplasm (Fig. 2b supplementary). Quantitation of p53 signals in immunostained cells showed UBXN2A overexpression can result in a significant (twofold) increase of nuclear p53 (Fig. 2c supplementary). Finally, immunostaining of LoVo colon cancer cells transiently co-transfected with GFP-empty/$(His)_6$-CHIP and GFP-UBXN2A/$(His)_6$-CHIP showed GFP-empty was unable to suppress CHIP-dependent destabilization of p53 (Fig. 3a and 3c supplementary). In contrast, GFP-UBXN2A antagonized CHIP-dependent destabilization of p53 resulting p53 relocalization to the nucleus (Fig. 3b and 3c supplementary). Ongoing projects in our group seek to further understand the mechanism behind the UBXN2A-mortalin-CHIP axis with and without stress in normal and cancerous cells.

UBXN2A interferes with cell proliferation and migration of colon cancer cells

It has already been shown that MKT-077, a cationic rhodacyanine dye analogue, can bind to mortalin protein within amino acids 252–310 and reverse the proliferative and anti-apoptotic functions of mortalin in cancer cells (Wadhwa et al. 2000). The same phenomena were observed in cancer cells when Kaul et al. (Kaul et al. 2005) used a p53 carboxyl-terminal peptide to block mortalin's binding pocket. We hypothesized that UBXN2A binding to mortalin's binding pocket can also disrupt mortalin's interaction with partners, antagonize oncogenic function of mortalin, and eventually induce cell cytotoxicity in cancer cells. Overexpression of mortalin correlates with a higher proliferation rate, colony forming efficacy, motility, and tumor forming capacity; poor survival; and increased resistance to therapies (Dundas et al. 2005; Gestl and Anne Bottger 2012; Guo et al. 2014; Sadekova et al. 1997).

To test the influence of UBXN2A on mortalin oncogenic function, we chose cell and colony proliferation assays as well as a cell migration assay in colon cancer cell lines. For the cell proliferation assay, we used an MTT assay in which we compared the proliferation rate of HCT-116 cells expressing $(His)_6$-empty vector or $(His)_6$-TYG-UBXN2A. Figure 4a shows expression of UBXN2A significantly decreases cell proliferation in a time-dependent manner. We particularly observed a negative growth in cells expressing UBXN2A in the first 24 h due to significant death in cells expressing a high level of UBXN2A protein. After the first 24 h, we observed cell growth in both empty and UBXN2A-expressing cells; however, the results showed that cells expressing exogenous UBXN2A still grew more slowly than the control cells under the same circumstances (Fig. 4a), as previously illustrated for other anti-cancer proteins (Yu et al. 2012). For the colony formation assay, HCT-116 colon cancer cells were transfected with $(His)_6$-empty vector or $(His)_6$-TYG-UBXN2A. After 48 h of antibiotic selection, cells were seeded for the colony formation assay. UBXN2A expression significantly decreased the amount of clones in HCT-116 cells when compared to cells expressing empty vector (Fig. 4b).

The current results indicate while UBXN2A expression has the ability to significantly decrease the number of colonies, some cells still keep the ability to form large colonies (Steinmetz et al. 1993). These colonies can be untransfected colonies or colonies with low-level expression of exogenous UBXN2A. Cells with high expression of UBXN2A enter into apoptosis 24 h after transfection or induction (Abdullah et al. 2015a; Sane et al. 2014). In addition, Lu et al. reported exogenous stresses, in this case Lipofectamine 2000 (Fiszer-Kierzkowska et al. 2011), can increase mortalin-p53 binding, resulting in elevation of cell proliferation (Lu et al. 2011). It is possible that the observed large colonies dominantly have a huge pool of mortalin-p53 resistant to UBXN2A anti-mortalin function.

Another factor that can explain the presence of large colonies in HCT-116 cells expressing UBXN2A is a phenomenon called stress-induced premature senescence (SIPS) induced by WT-p53 (Mirzayans et al. 2012). The SIPS cells can maintain viability and secrete factors that, among other detrimental effects, can promote tumor growth (Sliwinska et al. 2009). In addition, SIPS might not be a "permanent" growth-arrested state, and some SIPS cells can escape the proliferation block and give rise to aneuploid progeny that can re-enter the mitotic cycle as previously described in HCT-116 cells (Mirzayans et al. 2012). There are ongoing experiments in our group to determine whether overexpression of UBXN2A and its downstream effect on the p53 pathway may have a dual effect as follows: (1) UBXN2A can block the proliferation of the majority of the cancer cells though unsequestration of p53 and suppression of other tumorigenic partners of mortalin. (2) In contrast, UBXN2A-dependent activation of p53 can lead to the appearance of proliferating aneuploid cells capable of accelerating selective proliferation as previously described by Roninson et al. (Roninson 2003).

To evaluate whether interference with proliferation is also detected in other mitogen-dependent processes, we measured the influence of UBXN2A expression on cell migration. To

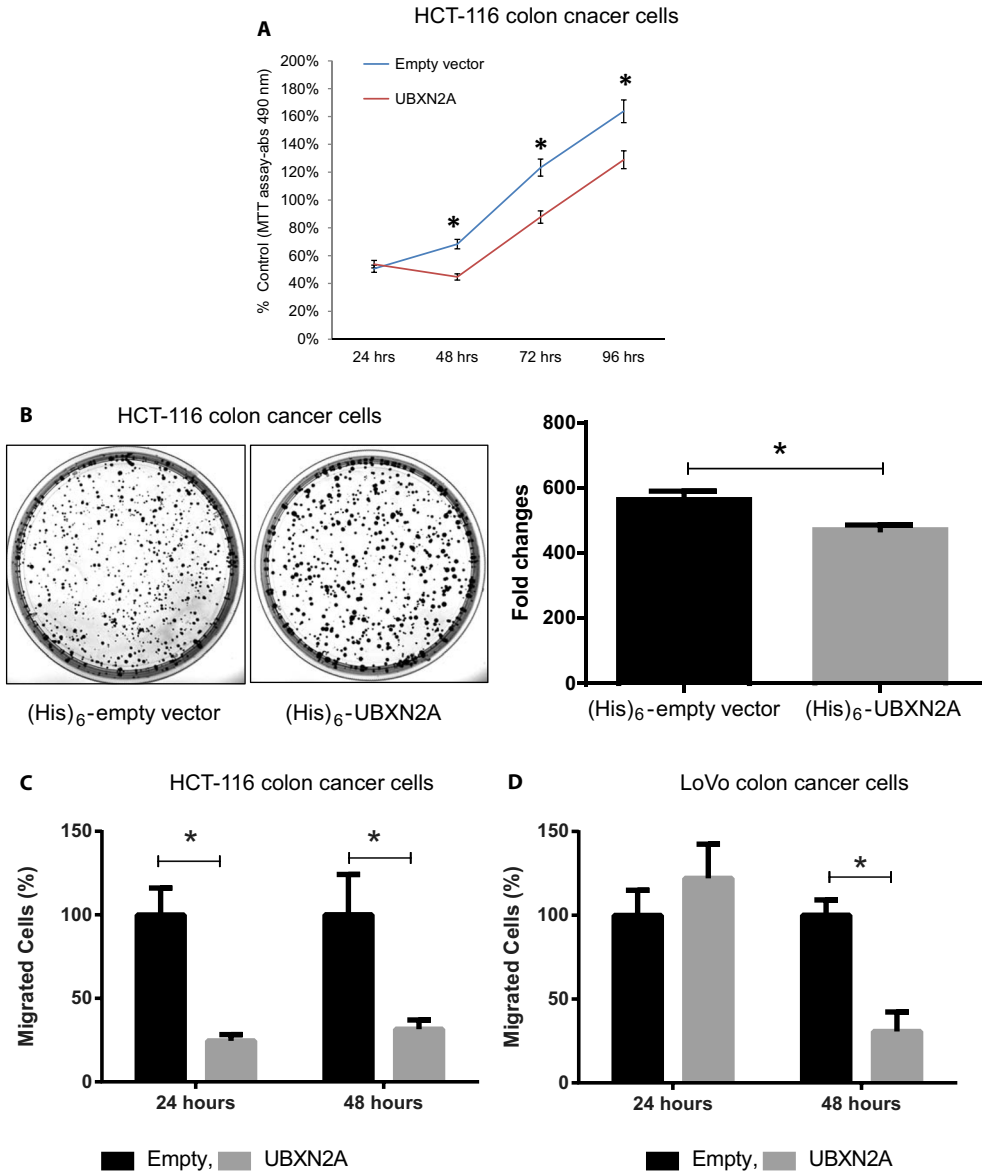

Fig. 4 UBXN2A expression suppresses cell proliferation and migration in colon cancer cells. **a** HCT-116 colon cancer cells transiently expressing $(His)_6$-empty and $(His)_6$-UBXN2A were seeded and subjected to an MTT cell proliferation assay at four different time points. The MTT assay revealed expression of UBXN2A particularly blocks cell proliferation in the first 24 h after transfection. UBXN2A continues its negative effect on cell proliferation after 48 h in comparison to cells expressing empty vector. **b** HCT-116 cancer cells transfected with $(His)_6$-empty and $(His)_6$-UBXN2A vector were selected with antibiotic (Zeocin, 100 μg/ml) for 48 h and seeded to plates for a colony formation assay (see material and method). Counted colonies showed while UBXN2A expression has the ability to significantly decrease the number of colonies, some cells keep the ability to form large colonies. (**c**, **d**) Poorly differentiated HCT-116 (**c**) and well-differentiated LoVo (**d**) colon cancer cells were transiently transfected with GFP-empty or GFP-UBXN2A followed by a cell migration assay (see "Material and methods" section). The cell migration assays in HCT-116 and LoVo cancer cells expressing GFP-empty or GFP-UBXN2A revealed that UBXN2A expression can significantly reduce cell migration, particularly 48 h post-transfection, regardless of the grade of cancer cells

this end, poorly differentiated HCT-116 and well-differentiated LoVo cells were transfected with GFP-empty or GFP-UBXN2A, and 48 h post-infection, a migration assay was performed (see Material and methods). The time to close the gap by migrated cells was significantly delayed when cells expressed UBXN2A (Fig. 4c–d).

shRNA knockdown of UBXN2A significantly reduces the cytotoxic effects of 5-FU in U2OS with enriched cytoplasmic mortalin

It has been shown that the human osteosarcoma U2OS cell line has enriched perinuclear mortalin protein, indicating

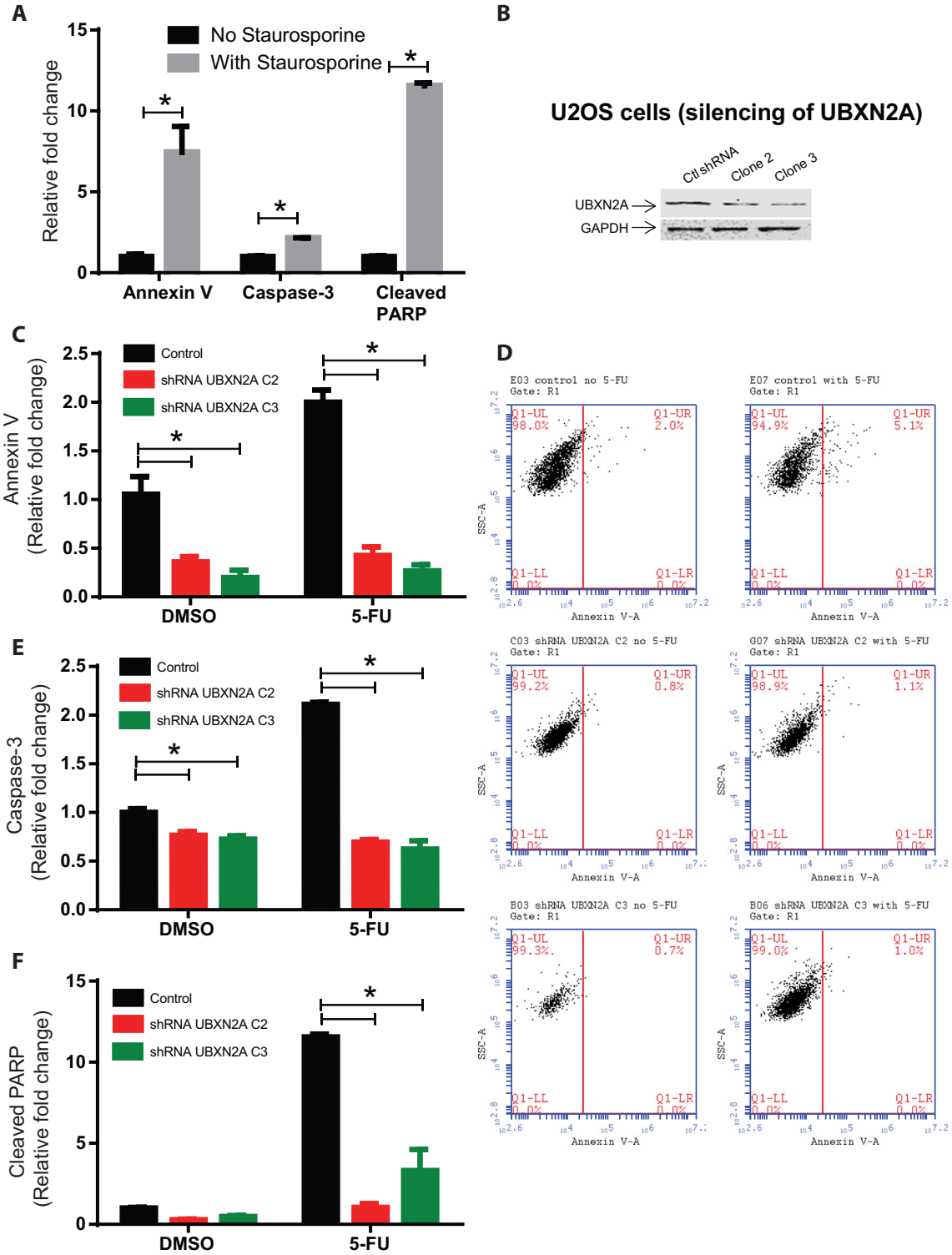

Fig. 5 shRNA knockdown of UBXN2A significantly reduces the cytotoxic effects of 5-FU in U2OS with enriched cytoplasmic mortalin. We used a human osteosarcoma U2OS cell line with enriched cytoplasmic mortalin to investigate whether inhibition of UBXN2A expression by interference RNA modulates 5-FU-induced apoptosis. **a** Twenty-four hours' incubation with staurosporine (50 nM positive control) successfully induced apoptosis in U2OS as measured by Annexin V, caspase-3, and cleaved PARP. **b** Transfection with shRNA lentiviral against UBXN2A generated two stable clones with efficient UBXN2A silencing (clones 2 and 3). (**c**–**f**) Cells stably expressing scrambled shRNA or shRNA against UBXN2A were treated with vehicle or 5-FU (100 μM) for 48 h followed by flow cytometry using Annexin V (**c**, **d**), caspase-3 (**e**), and cleaved PARP (**f**) apoptotic markers ($n=6$, $P<0.05$). Spontaneous apoptosis seen in the absence of 5-FU has been described previously. Results indicate UBXN2A silencing can inhibit 5-FU-induced apoptotic events

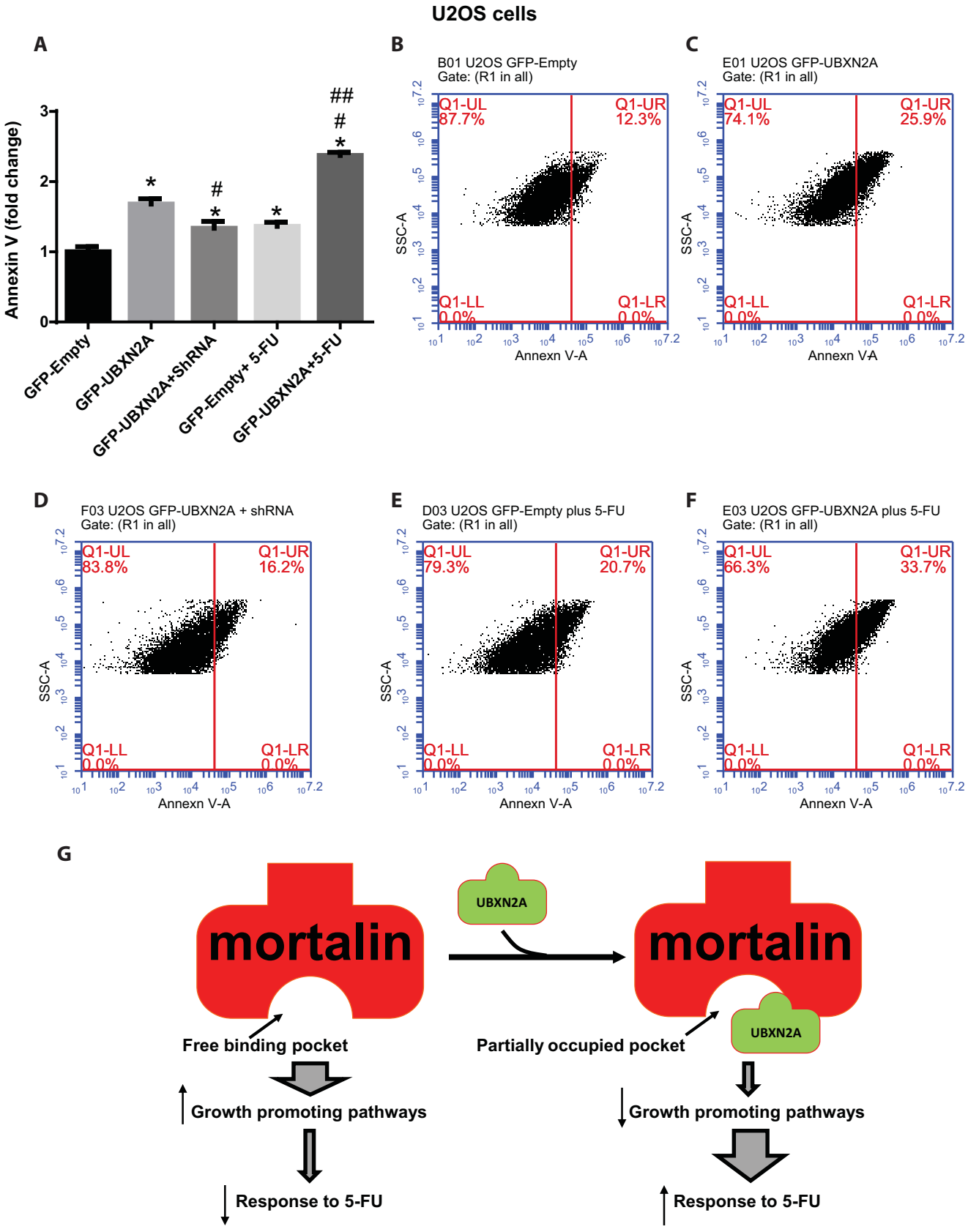
U2OS cells
A
Annexin V (fold change)
GFP-Empty
GFP-UBXN2A
GFP-UBXN2A+ShRNA
GFP-Empty+ 5-FU
GFP-UBXN2A+5-FU
B
B01 U2OS GFP-Empty
Gate: (R1 in all)
Q1-UL 87.7%
Q1-UR 12.3%
Q1-LL 0.0%
Q1-LR 0.0%
SSC-A
Annexn V-A
C
E01 U2OS GFP-UBXN2A
Gate: (R1 in all)
Q1-UL 74.1%
Q1-UR 25.9%
Q1-LL 0.0%
Q1-LR 0.0%
D
F03 U2OS GFP-UBXN2A + shRNA
Gate: (R1 in all)
Q1-UL 83.8%
Q1-UR 16.2%
Q1-LL 0.0%
Q1-LR 0.0%
E
D03 U2OS GFP-Empty plus 5-FU
Gate: (R1 in all)
Q1-UL 79.3%
Q1-UR 20.7%
Q1-LL 0.0%
Q1-LR 0.0%
F
E03 U2OS GFP-UBXN2A plus 5-FU
Gate: (R1 in all)
Q1-UL 66.3%
Q1-UR 33.7%
Q1-LL 0.0%
Q1-LR 0.0%
G
mortalin
UBXN2A
mortalin
Free binding pocket
Partially occupied pocket
UBXN2A
Growth promoting pathways
Growth promoting pathways
Response to 5-FU
Response to 5-FU

◀ **Fig. 6** Overexpression of UBXN2A induces apoptosis in U2OS and enhances apoptotic events induced by 5-FU. (**a**–**f**) U2OS were (co)-transfected with GFP-empty, GFP-UBXN2A, or GFP-UBXN2A plus lentiviral shRNA against UBXN2A (used for clone 3 in Fig. 5) and treated with and without 5-FU (100 μM) for 48 h. Cells were collected and subjected to Annexin V (BD Biosciences) staining for flow cytometry. Using the BD Accuri C6 Software, GFP-expressing cells were first gated and then Annexin V-positive cells were plotted. The average Annexin V binding measured in control and treated cells (**a**) showed UBXN2A is a pro-apoptotic protein (dot plot diagram c versus b and d). More importantly, GFP-UBXN2A expression enhances the apoptotic function of 5-FU (dot plot diagram f versus e). Graphs show the mean± standard error of the results of six independent experiments. **g** The proposed mechanism of action of UBXN2A in mortalin-enriched cancer cells such as osteosarcoma. Oncoprotein mortalin and its binding protein partners promote cancer growth and decrease cell response to 5-FU chemotherapy. By binding to SBD's binding pocket, UBXN2A inhibits mortalin function, induces apoptosis, and consequently increases the cytotoxic effect of conventional chemotherapy

mortalin is a predominant oncoprotein in this cancer cell line (Widodo et al. 2007) similar to colon cancer cells. In fact, mortalin knockdown decreases growth in U2OS (Kaul et al. 2003; Ran et al. 2000; Wadhwa et al. 1993a). Based on this evidence, we chose U2OS as an ideal model for examining the apoptotic events in the presence and the absence of UBXN2A. We first examined whether three common apoptotic events (Annexin V, caspase-3, and cleaved PARP) are present in U2OS in response to staurosporine, a well-known inducer of apoptosis in a wide range of cell lines (Belmokhtar et al. 2001). Figure 5a shows staurosporine induces early-stage apoptosis measured by Annexin V as well as caspase-3 and PARP cleavages after 48 h. Using lentiviral shRNA, we stably silenced UBXN2A in U2OS cells. Figure 5b shows efficient silencing of UBXN2A in clones 2 and 3 versus cells expressing scrambled shRNA. The U2OS control group and clones 2 and 3 were treated with DMSO (0.1 % final concentration) or 5-FU (100 μM) (Eby et al. 2010) for 48 h, followed by flow cytometry using an early apoptosis marker, Annexin V (Abdullah et al. 2015a). We recorded a spontaneous apoptosis (Ehemann et al. 2003; Wang et al. 1996) in DMSO-treated cells, which was suppressed in the absence of UBXN2A (Fig. 5c). On the other hand, treatment of cells with an oncogenic agent, 5-FU, led to a significant apoptosis in control cells, while clones 2 and 3 expressing UBXN2A shRNA showed no elevation of Annexin V in response to 5-FU (Fig. 5c, d). In panels e and f of Fig. 5, cells treated with DMSO or 5-FU for 48 h were then subjected to flow cytometry using caspase-3 Alexa Fluor® 647 or anti-cleaved PARP+ secondary fluorescent Alexa Fluor® 546 antibody. While 5-FU significantly induced the elevation of caspase-3 (Figs. 5e and 4a-c supplementary) and cleaved PARP (Figs. 5f and 4d–f supplementary) in cells expressing scrambled shRNA, 5-FU failed to increase caspase-3 or cleaved PARP in shRNA-silenced clones 2 and 3. Together, these results indicate UBXN2A can mediate the apoptosis events induced by 5-FU in U2OS cells.

UBXN2A enhances the cytotoxicity of a chemotherapeutic agent, 5-FU, in an osteosarcoma cell line

The experiments conducted in Fig. 5 demonstrated that UBXN2A depletion can decrease 5-FU-induced apoptosis assessed by Annexin V as well as caspase-3 and PARP cleavages. To better understand the mechanisms whereby UBXN2A induces apoptosis, we transfected human osteosarcoma U2OS cells with GFP-UBXN2A. In this gain-of-function approach, we examined whether overexpression of UBXN2A can increase the cytotoxic effect of 5-FU. Cells were transiently transfected with the GFP-empty or GFP-UBXN2A capable to bind to mortalin (Sane et al. 2014). Overexpression of UBXN2A and not empty vector successfully induced early apoptosis in U2OS (Fig. 6a–c). In addition, another group of cells was co-transfected with GFP-UBXN2A and lentiviral shRNA against UBXN2A (used in Fig. 5b). Coexpression of UBXN2A shRNA in cells antagonized the pro-apoptotic function of exogenous UBXN2A (Fig. 6a, d), illustrated by the reduction of Annexin V. Together, this set of experiments confirmed that UBXN2A can act as a pro-apoptotic protein in U2OS. Finally, we examined the level of Annexin V apoptosis marker in transfected cells treated with 5-FU (100 μM) for 48 h. As a genotoxic agent, 5-FU successfully increased Annexin V levels in cells expressing GFP-empty cells (Fig. 6a, e). However, the presence of exogenous UBXN2A significantly elevated the 5-FU-induced apoptosis (Fig. 6a, f). Taken together, UBXN2A expression in combination with a genotoxic agent appears to be a promising strategy for the treatment of human U2OS osteosarcoma cells. An ongoing project in our lab endeavors to repeat these results in a U2OS xenograft mouse model treated with a combination of UBXN2A enhancer (Abdullah et al. 2015a) and 5-FU.

Discussion

Osteosarcoma is the most common primary malignant bone cancer in children and adolescents. Particularly, osteosarcoma is aggressive in children despite surgery and chemotherapy and is prone to relapse (Marina et al. 2004). A recent improvement in chemotherapeutic regimens has increased the long-term survival rate (Kim et al. 2010; Tang et al. 2011). However, these patients still have a poor response to chemotherapy, which is usually associated with a poor prognosis (Basu-Roy et al. 2013). Therefore, there is an emerging demand for novel therapeutic approaches for patients with osteosarcoma (Hattinger et al. 2010; Kim and Helman 2009). This current study introduces the identification of a novel anti-cancer pathway that can improve the

responses of tumorigenic cells to classic chemotherapy in patients with osteosarcoma.

A set of molecular modeling and protein-protein docking studies clearly demonstrate that mortalin's binding pocket, located in the SBD domain of the protein, is able to accommodate the SEP domain of UBXN2A. In addition, this computational study suggested the essential presence of PRO442, LYS555, and ILE558 within mortalin's binding pocket and their relation with the SEP domain of UBXN2A protein. While further studies such as a protein crystallization technique are necessary to determine UBXN2A-mortalin protein complexes at atomic resolution, this simulation reveals a dynamic and stable binding pocket within the SBD domain of mortalin in which the SEP domain of UBXN2A can bind. We believe the initial binding of the SEP domain leads to the formation of further affinity- and specificity-increasing interactions between the additional domain of UBXN2A and mortalin's binding pocket. More importantly, this current structure study suggests a section of the p53 binding site on mortalin protein structurally is the matching pocket for the SEP domain of UBXN2A.

It has been shown that mutation in specific residues within the binding pocket of HSP70 protein can disable HSP70 from binding to a selective substrate (Rohrer et al. 2014). Completion of Y2H and IP experiments confirmed PRO442, LYS555, and ILE558 are essential residues in the mortalin pocket when the SEP domain binds to the SBD domain of mortalin. In previous Y2H experiments (Sane et al. 2014). truncated forms of mortalin suggested a section of the SBD domain between 438 and 506 residues is essential for UBXN2A binding. However, in those truncated forms, we kept ATP at the N-terminus of truncated SBD. In this current study, we eliminated the ATP domain to better understand how SBD's pocket meditates UBXN2A-mortalin interactions.

It has been previously reported that the N-terminal of mortalin (253–282) is important for p53 binding (Kaul et al. 2001; Wadhwa et al. 2000). However, another set of studies showed p53 binds to the substrate-binding site located at the C-terminus of mortalin (Iosefson and Azem 2010; Utomo et al. 2012). The differences between the above results are certainly explained by possible modification or additional interacting partners observed in the in vitro and in vivo systems utilized in the above reports.

Our structural studies (Fig. 1) as well as the Y2H and pull-down experiments (Figs. 2 and 3) presented in this current study combined with our previous results (Sane et al. 2014) suggest both the N-terminus and C-terminus of mortalin contribute to UBXN2A interaction, similar to p53 and MKT-077 binding to mortalin (Grover et al. 2012; Wadhwa et al. 2000). These current results suggest the following facts: (1) UBXN2A binds to mortalin's substrate pocket located in the C-terminus, and this binding can be affected by the absence of PRO442, LYS555, and ILE558 amino acids as well as the presence of the N-terminus of mortalin (1–506 aa) (Sane et al. 2014). (2) Binding of UBXN2A to the substrate-binding pocket masks a part of the p53 binding site within the substrate-binding domain of mortalin (THR433, VAL435, LEU436, LEU437, PRO442, ILE558, LYS555) (Utomo et al. 2012). (3) UBXN2A's binding to the substrate-binding pocket may lead to conformational changes (Sharma and Masison 2009; Zhuravleva and Gierasch 2015) in the N-terminus (ATPase domain) of mortalin, which is also critical for p53's binding to mortalin (Kaul et al. 2001). (4) Other sections of mortalin domain such as the ATP and lid domains can be used as the second site of interaction with UBXN2A. Similar multi-interaction sites were described for UBXD1 protein when it binds to p97 protein platform (Kern et al. 2009). Together, the above results confirmed UBXN2A is a regulatory partner of mortalin and UBXN2A uses the SEP domain to fit and bind to the SBD conserved pocket.

This current study suggests UBXN2A binds to mortalin's protein binding pocket and interferes with mortalin's binding partners (Dundas et al. 2005; Gestl and Anne Bottger 2012; Guo et al. 2014; Sadekova et al. 1997) resulting in inactivation of mortalin oncoprotein in cancer cells. Part of the apoptotic resistance of cancer cells is mediated by activation of WT-mortalin in cancer cells, including osteosarcoma (Wadhwa et al. 2015). therefore, inhibition of this mortalin-induced survival response by UBXN2A may be an important adjunct to increase the efficacy of chemotherapy. Further studies are required to dissect the various mechanisms underlying UBXN2A anti-cancer functions upon its binding to mortalin and how UBXN2A-dependent inhibition of the mortalin oncoprotein pathway can alter the apoptotic efficacy of chemotherapy (Fig. 6g). The tumor cells use several molecular mechanisms to suppress apoptosis and acquire resistance to classic chemotherapies. An increasing number of studies have clearly established that mortalin is a dominant oncoprotein in several solid tumors affecting both anti-apoptotic and pro-apoptotic proteins (Deocaris et al. 2013; Yoo et al. 2010). Completion of this study showed UBXN2A can bind and inhibit mortalin oncoprotein, resulting in induction of the apoptosis pathway in the presence of 5-FU. Therefore, UBXN2A can be targeted to stimulate apoptosis in solid tumors with high levels of mortalin.

In summary, the additive effect of a pro-apoptotic UBXN2A and the cytotoxic anti-cancer function of 5-FU could be an effective treatment strategy, particularly for those mortalin-enriched tumors such as osteosarcoma. Induced UBXN2A (Abdullah et al. 2015a) can inhibit mortalin oncoprotein, which is required for the development of osteosarcoma tumors. This approach may improve the efficacy of classic chemotherapies and lead to better management of patient survivors.

Acknowledgments This project has been funded by the KR start-up package provided by the Division of Basic Biomedical Sciences, University of South Dakota. In addition, it was partially covered by the National Institute of General Medical Sciences of the National Institutes of Health under award number 5P20GM103548 (Miskimins) and the SD Biomedical Research Infrastructure Network (SD BRIN) program of the NIH/NIGMS IDeA Networks of Biomedical Research Excellence (INBRE) program. We appreciate the essential technical supports provided to the project by BK. Gupta.

Compliance with ethical standards

Competing interests The authors declare that they have no competing interests.

References

Abdullah A, Sane S, Branick KA, Freeling JL, Wang H, Zhang D, Rezvani K (2015a) A plant alkaloid, veratridine, potentiates cancer chemosensitivity by UBXN2A-dependent inhibition of an oncoprotein, mortalin-2 Oncotarget 6(27):23561–23581

Abdullah A, Sane S, Freeling JL, Wang H, Zhang D, Rezvani K (2015b) Nucleocytoplasmic translocation of UBXN2A is required for apoptosis during DNA damage stresses in colon cancer cells. J Cancer 6:1066–1078

Arnold K, Bordoli L, Kopp J, Schwede T (2006) The SWISS-MODEL workspace: a web-based environment for protein structure homology modelling. Bioinformatics 22:195–201

Basu-Roy U, Basilico C, Mansukhani A (2013) Perspectives on cancer stem cells in osteosarcoma. Cancer Lett 338:158–167

Belmokhtar CA, Hillion J, Segal-Bendirdjian E (2001) Staurosporine induces apoptosis through both caspase-dependent and caspase-independent mechanisms. Oncogene 20:3354–3362

Bhattacharya A, Tejero R, Montelione GT (2007) Evaluating protein structures determined by structural genomics consortia. Proteins 66:778–795

Biasini M et al (2014) SWISS-MODEL: modelling protein tertiary and quaternary structure using evolutionary information. Nucleic Acids Res 42:W252–258

Chen J et al (2014) Overexpression of mortalin in hepatocellular carcinoma and its relationship with angiogenesis and epithelial to mesenchymal transition. Int J Oncol 44:247–255

Comeau SR, Gatchell DW, Vajda S, Camacho CJ (2004) ClusPro: an automated docking and discrimination method for the prediction of protein complexes. Bioinformatics 20:45–50

Conte M, Deri P, Isolani ME, Mannini L, Batistoni R (2009) A mortalin-like gene is crucial for planarian stem cell viability. Dev Biol 334: 109–118

Deocaris CC, Lu WJ, Kaul SC, Wadhwa R (2013) Druggability of mortalin for cancer and neuro-degenerative disorders. Curr Pharm Des 19:418–429

Dundas SR, Lawrie LC, Rooney PH, Murray GI (2005) Mortalin is overexpressed by colorectal adenocarcinomas and correlates with poor survival. J Pathol 205:74–81

Eby KG et al (2010) ISG20L1 is a p53 family target gene that modulates genotoxic stress-induced autophagy. Mol Cancer 9:95

Ehemann V, Sykora J, Vera-Delgado J, Lange A, Otto HF (2003) Flow cytometric detection of spontaneous apoptosis in human breast cancer using the TUNEL-technique. Cancer Lett 194:125–131

Esser C, Scheffner M, Hohfeld J (2005) The chaperone-associated ubiquitin ligase CHIP is able to target p53 for proteasomal degradation. J Biol Chem 280:27443–27448

Fiszer-Kierzkowska A, Vydra N, Wysocka-Wycisk A, Kronekova Z, Jarzab M, Lisowska KM, Krawczyk Z (2011) Liposome-based DNA carriers may induce cellular stress response and change gene expression pattern in transfected cells. BMC Mol Biol 12:27

Gestl EE, Anne Bottger S (2012) Cytoplasmic sequestration of the tumor suppressor p53 by a heat shock protein 70 family member, mortalin, in human colorectal adenocarcinoma cell lines. Biochem Biophys Res Commun 423:411–416

Grover A et al (2012) Withanone binds to mortalin and abrogates mortalin-p53 complex: computational and experimental evidence. Int J Biochem Cell Biol 44:496–504

Guo W et al (2014) Targeting GRP75 improves HSP90 inhibitor efficacy by enhancing p53-mediated apoptosis in hepatocellular carcinoma. PLoS One 9:e85766

Hattinger CM, Pasello M, Ferrari S, Picci P, Serra M (2010) Emerging drugs for high-grade osteosarcoma. Expert Opin Emerg Drugs 15: 615–634. doi:10.1517/14728214.2010.505603

Iosefson O, Azem A (2010) Reconstitution of the mitochondrial Hsp70 (mortalin)-p53 interaction using purified proteins—identification of additional interacting regions. FEBS Lett 584:1080–1084. doi:10.1016/j.febslet.2010.02.019

Kaul SC, Reddel RR, Mitsui Y, Wadhwa R (2001) An N-terminal region of mot-2 binds to p53 in vitro. Neoplasia 3:110–114

Kaul Z, Yaguchi T, Kaul SC, Hirano T, Wadhwa R, Taira K (2003) Mortalin imaging in normal and cancer cells with quantum dot immuno-conjugates. Cell Res 13:503–507

Kaul SC, Aida S, Yaguchi T, Kaur K, Wadhwa R (2005) Activation of wild type p53 function by its mortalin-binding, cytoplasmically localizing carboxyl terminus peptides. J Biol Chem 280:39373–39379. doi:10.1074/jbc.M500022200

Kaul SC, Deocaris CC, Wadhwa R (2007) Three faces of mortalin: a housekeeper, guardian and killer. Exp Gerontol 42:263–274. doi:10.1016/j.exger.2006.10.020

Kern M, Fernandez-Saiz V, Schafer Z, Buchberger A (2009) UBXD1 binds p97 through two independent binding sites. Biochem Biophys Res Commun 380:303–307

Kim SY, Helman LJ (2009) Strategies to explore new approaches in the investigation and treatment of osteosarcoma. Cancer Treat Res 152: 517–528

Kim HJ, Chalmers PN, Morris CD (2010) Pediatric osteogenic sarcoma. Curr Opin Pediatr 22:61–66

Kozakov D, Beglov D, Bohnuud T, Mottarella SE, Xia B, Hall DR, Vajda S (2013) How good is automated protein docking? Proteins 81: 2159–2166

Krieger E, Vriend G (2015) New ways to boost molecular dynamics simulations. J Comput Chem 36:996–1007

Krieger E, Dunbrack RL Jr, Hooft RW, Krieger B (2012) Assignment of protonation states in proteins and ligands: combining pKa prediction with hydrogen bonding network optimization. Methods Mol Biol 819:405–421

Lee JT, Gu W (2010) The multiple levels of regulation by p53 ubiquitination. Cell Death Differ 17:86–92. doi:10.1038/cdd.2009.77

Lu WJ, Lee NP, Kaul SC, Lan F, Poon RT, Wadhwa R, Luk JM (2011) Mortalin-p53 interaction in cancer cells is stress dependent and constitutes a selective target for cancer therapy. Cell Death Differ 6: 1046–1056. doi:10.1038/cdd.2010.177

Marina N, Gebhardt M, Teot L, Gorlick R (2004) Biology and therapeutic advances for pediatric osteosarcoma. Oncologist 9:422–441

Mirzayans R, Andrais B, Scott A, Murray D (2012) New insights into p53 signaling and cancer cell response to DNA damage: implications for cancer therapy. J Biomed Biotechnol 2012:170325

Qian SB, McDonough H, Boellmann F, Cyr DM, Patterson C (2006) CHIP-mediated stress recovery by sequential ubiquitination of substrates and Hsp70. Nature 440:551–555

Ran Q et al (2000) Extramitochondrial localization of mortalin/mthsp70/PBP74/GRP75. Biochem Biophys Res Commun 275:174–179

Rezvani K et al (2009) UBXD4, a UBX-containing protein, regulates the cell surface number and stability of alpha3-containing nicotinic acetylcholine receptors. J Neurosci 29:6883–6896. doi:10.1523/JNEUROSCI.4723-08.2009

Rezvani K et al (2012) Proteasomal degradation of the metabotropic glutamate receptor 1alpha is mediated by Homer-3 via the proteasomal S8 ATPase: signal transduction and synaptic transmission. J Neurochem 122:24–37

Rohrer KM, Haug M, Schworer D, Kalbacher H, Holzer U (2014) Mutations in the substrate binding site of human heat-shock protein 70 indicate specific interaction with HLA-DR outside the peptide binding groove. Immunology 142:237–247

Roninson IB (2003) Tumor cell senescence in cancer treatment. Cancer Res 63:2705–2715

Ryu J et al (2014) Identification and functional characterization of nuclear mortalin in human carcinogenesis. J Biol Chem 289:24832–24844

Sadekova S, Lehnert S, Chow TY (1997) Induction of PBP74/mortalin/Grp75, a member of the hsp70 family, by low doses of ionizing radiation: a possible role in induced radioresistance. Int J Radiat Biol 72:653–660

Sane S et al (2014) Ubiquitin-like (UBX)-domain-containing protein, UBXN2A, promotes cell death by interfering with the p53-Mortalin interactions in colon cancer cells. Cell Death Dis 5:e1118

Sharma D, Masison DC (2009) Hsp70 structure, function, regulation and influence on yeast prions. Protein Pept Lett 16:571–581

Sliwinska MA et al (2009) Induction of senescence with doxorubicin leads to increased genomic instability of HCT116 cells. Mech Ageing Dev 130:24–32

Soukenik M et al (2004) The SEP domain of p47 acts as a reversible competitive inhibitor of cathepsin L. FEBS Lett 576:358–362

Steinmetz KA, Potter JD, Folsom AR (1993) Vegetables, fruit, and lung cancer in the Iowa Women's Health Study. Cancer Res 53:536–543

Tai-Nagara I, Matsuoka S, Ariga H, Suda T (2014) Mortalin and DJ-1 coordinately regulate hematopoietic stem cell function through the control of oxidative stress. Blood 123:41–50

Tang QL et al (2011) Enrichment of osteosarcoma stem cells by chemotherapy. Chin J Cancer 30:426–432

Teng Y, Rezvani K, De Biasi M (2015) UBXN2A regulates nicotinic receptor degradation by modulating the E3 ligase activity of CHIP. Biochem Pharmacol 97(4):518–530. doi:10.1016/j.bcp.2015.08.084

Utomo DH, Widodo N, Rifa'i M (2012) Identifications small molecules inhibitor of p53-mortalin complex for cancer drug using virtual screening. Bioinformation 8:426–429

Wadhwa R, Kaul SC, Mitsui Y, Sugimoto Y (1993a) Differential subcellular distribution of mortalin in mortal and immortal mouse and human fibroblasts. Exp Cell Res 207:442–448

Wadhwa R, Kaul SC, Sugimoto Y, Mitsui Y (1993b) Induction of cellular senescence by transfection of cytosolic mortalin cDNA in NIH 3T3 cells. J Biol Chem 268:22239–22242

Wadhwa R et al (2000) Selective toxicity of MKT-077 to cancer cells is mediated by its binding to the hsp70 family protein mot-2 and reactivation of p53 function. Cancer Res 60:6818–6821

Wadhwa R, Takano S, Kaur K, Deocaris CC, Pereira-Smith OM, Reddel RR, Kaul SC (2006) Upregulation of mortalin/mthsp70/Grp75 contributes to human carcinogenesis. Int J Cancer 118:2973–2980

Wadhwa R, Ryu J, Ahn HM, Saxena N, Chaudhary A, Yun CO, Kaul SC (2015) Functional significance of point mutations in stress chaperone mortalin and their relevance to Parkinson disease. J Biol Chem 290:8447–8456

Wang C, Eshleman J, Lutterbaugh J, Bin Y, Willson J, Markowitz S (1996) Spontaneous apoptosis in human colon tumor cell lines and the relation of wt p53 to apoptosis. Chin Med J (Engl) 109:537–541

Widodo N et al (2007) Stress chaperones, mortalin, and pex19p mediate 5-aza-2′ deoxycytidine-induced senescence of cancer cells by DNA methylation-independent pathway. J Gerontol A Biol Sci Med Sci 62:246–255

Wu PK, Hong SK, Veeranki S, Karkhanis M, Starenki D, Plaza JA, Park JI (2013) A mortalin/HSPA9-mediated switch in tumor-suppressive signaling of Raf/MEK/extracellular signal-regulated kinase. Mol Cell Biol 33:4051–4067

Yang L et al (2011) Crosstalk between Raf/MEK/ERK and PI3K/AKT in suppression of Bax conformational change by Grp75 under glucose deprivation conditions. J Mol Biol 414:654–666

Yoo JY, Ryu J, Gao R, Yaguchi T, Kaul SC, Wadhwa R, Yun CO (2010) Tumor suppression by apoptotic and anti-angiogenic effects of mortalin-targeting adeno-oncolytic virus. J Gene Med 12:586–595

Yu W, Wang Y, Gong M, Pei F, Zheng J (2012) Phosphoprotein associated with glycosphingolipid microdomains 1 inhibits the proliferation and invasion of human prostate cancer cells in vitro through suppression of Ras activation. Oncol Rep 28:606–614

Yuan J, Luo K, Zhang L, Cheville JC, Lou Z (2010) USP10 regulates p53 localization and stability by deubiquitinating p53. Cell 140:384–396. doi:10.1016/j.cell.2009.12.032

Zhuravleva A, Gierasch LM (2015) Substrate-binding domain conformational dynamics mediate Hsp70 allostery. Proc Natl Acad Sci U S A 112:E2865–2873